## Cellular automata as convolutional neural networks

William Gilpin\*
Department of Applied Physics, Stanford University

(Dated: June 23, 2022)

Deep learning techniques have recently demonstrated broad success in predicting complex dynamical systems ranging from turbulence to human speech—motivating broader questions about how neural networks encode and represent dynamical rules. We explore this problem in the context of cellular automata (CA), simple dynamical systems that are intrinsically discrete and thus difficult to analyze using standard tools from dynamical systems theory. We show that any CA may readily be represented using a convolutional neural network with a network-in-network architecture. This motivates our development of a general convolutional multilayer perceptron architecture, which we find can learn the dynamical rules for arbitrary CA when given videos of the CA as training data. In the limit of large network widths, we find that training dynamics are strongly stereotyped across replicates, and that common patterns emerge in the structure of networks trained on different CA rulesets. We train ensembles of networks on randomly-sampled CA, and we probe how the trained networks internally represent the CA rules using an information-theoretic technique based on distributions of layer activation patterns. We find that CA with simpler rule tables produce trained networks with hierarchical structure and layer specialization, while more complex CA tend to produce shallower representations—illustrating how the underlying complexity of the CA's rules influences the specificity of these internal representations. Our results suggest how the entropy of a physical process can affect its representation when learned by neural networks.

Recent studies have demonstrated the surprising ability of deep neural networks to learn predictive representations of dynamical systems [1-5]. For example, certain types of recurrent neural networks, when trained on short-timescale samples of a high-dimensional chaotic process, can learn transition operators for that process that rival traditional simulation techniques [2, 6, 7]. More broadly, neural networks can learn and predict general features of dynamical systems—ranging from turbulent energy spectra [8], to Hamiltonian ground states [9, 10], to topological invariants [11]. Such successes mirror wellknown findings in applied domains [12], which have convincingly demonstrated that neural networks may not only represent, but also learn, generators for processes ranging from speech generation [13] to video prediction [14]. However, open questions remain about how the underlying structure of a physical process affects its representation by a neural network trained using standard optimization techniques.

We aim to study such questions in the context of cellular automata (CA), among the simplest dynamical systems due to the underlying discreteness of both their domain and the dynamical variables that they model. The most widely-known CA is Conway's Game of Life, which consists of an infinite square grid of sites ("cells") that can only take on a value of zero ("dead") or one ("alive"). Starting from an initial binary pattern, each cell is synchronously updated based on its current state, as well as its current number of living and non-living neighbors. Despite its simple dynamical rules, the Game of Life has been found to exhibit remarkable properties

ranging from self-replication to Turing universality [15]. Such versatility offers a vignette of broader questions in CA research, because many CA offer minimal examples of complexity emerging from apparent simplicity [16–18]. For this reason, CA have previously been natural candidates for evaluating the expressivity and capability of machine learning techniques such as genetic algorithms [19, 20].

Here, we show that deep convolutional neural networks are capable of representing arbitrary cellular automata, and we demonstrate an example network architecture that smoothly and repeatably learns an arbitrary CA using standard loss gradient-based training. Our approach takes advantage of the "mean field limit" for large networks [21–23], for which we find that trained networks express a universal sparse representation of the CA based on depthwise consolidation of similar inputs.

We begin by making an explicit connection between cellular automata and neural networks. We define a CA as a dynamical system with M possible states that updates its value based on its current value and D other cells, usually its immediate neighbors in a square lattice. There are  $M^D$  possible unique M-ary input strings to a CA function, which we individually refer to as  $\sigma$ . A cellular automaton is fully specified by a transition ruleset  $\sigma \to m, m \in \{0, 1, ..., M\}$ , and there are  $M^{M^D}$  possible unique CA rulesets. For the Game of Life, M=2, D=9, and so the rule table consists of a Boolean function that maps each of the  $2^9 = 512$  possible 9-bit input strings to a single bit. A defining feature of CA is the locality of dynamical update rule, which ensures that the rule domain is small; the size of D thus sets an upper bound on the rate at which information propagates across space. This locality makes CA explicitly analogous to a convolutional

<sup>\*</sup> wgilpin@stanford.edu

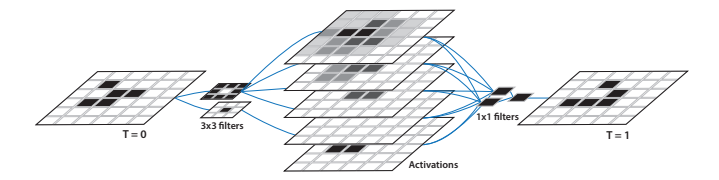


Figure 1. Conway's Game of Life as a convolutional neural network. Two convolutional filters identify the value of the center pixel and count the number of neighbors. These features are then scored and summed to generate a prediction for the system at the next timepoint.

neural network (CNN), the de facto standard neural network architecture for the analysis of images or highdimensional data [12]. In CNN, a trainable "kernel" is applied across input data though a series of local convolutions. The receptive field of these convolutional neurons is equivalent to the neighborhood D of the CA. These filters act as context-aware feature extractors; deeper layers thus need to consolidate the information these filters generate about a given neighborhood (and thus  $\sigma$ ) into a prediction for the output image (and thus m). This process can be implemented locally using successive  $1 \times 1$  convolutions, which recent applications of CNNs have shown to greatly increase network expressivity at low computational cost [24]. Because CA are explicitly local, the network requires no pooling layers—making the network the equivalent of fitting a small, convolutional multilayer perceptron or "mlpconv" to the CA [24, 25]. The appropriate weights to implement a given CA can actually be inferred analytically without the use of algorithmic training (Supplementary Material); one possible approach is to define a shallow network that uniquely matches each of the  $M^D$  input  $\sigma$  against a template, while another approach treats layers of the network like levels in a tree search that iteratively narrows down each input  $\sigma$  to the desired output m.

Figure 1 shows an example analytical mlpconv representation of the Game of Life, in which the two salient features for determining the CA evolution (the center pixel value and the number of neighbors) are extracted via an initial  $3 \times 3$  convolution, the results of which are passed to additional  $1 \times 1$  convolutional layers in order to generate a final output prediction (exact weights are given in Supplementary Material). The number of separate convolutions (four with the neighbor filter with different biases, and one with the identity filter) is affected by our choice of ReLU activations (the current best practice for deep convolutional networks) instead of traditional neurons with saturating nonlinearities [26]. Many alternative and equivalent representations may be defined, underscoring the expressivity of multilayer perceptrons when representing simple functions like CA.

Now assured that arbitrary cellular automata may be represented by convolutional perceptrons with finite layers and units, we ask whether automated training of neural networks on time series of cellular automata images is

sufficient to learn their rules. We investigate this process by training ensembles of convolutional neural networks on random random images and random CA rulesets. We start by defining a CA as an explicit mapping between each of  $2^9 = 512$  possible  $3 \times 3$  pixel groups in a binary image, and a single output pixel value. We then apply this map to an ensemble of random binary images (the training data), in order to produce a new output binary image set (the training labels). Here, we use large enough images ( $10 \times 10$  pixels) and training data batches (500 images) to ensure that the training data contains at least one instance of each rule. On average, each image contains an equal number of black and white pixels; for sufficiently large images this ensures that each of the 512 input states is equally probable. We note that, in principle, training the network will proceed much faster if the network is shown an example of only one rule at a time. However, such a process causes the network structure to depend strongly on the order in which individual rules were shown, whereas presenting all input cases simultaneously forces the network to learn internal rule representations based on their relative importance for maximizing accuracy.

Our network topology consists of a basic mlpconv architecture corresponding to a single  $3\times 3$  convolutional layer followed by a variable number of  $1\times 1$  layers [25]. The final layer consists of a uniform summation that generate a predicted value for the next state of a lattice site. Adding final "prediction" layer with softmax classifier accelerates training on binary CA by reducing the dependence of convergence on initial neuron weights; however we omit this step here in order to allow the same architecture to readily be generalized for CA with M>2. Our network may thus be considered a convolutional linear committee machine.

For the random initial conditions used, the Adam optimizer with an L2 norm loss function was used with hyperparameters (training rate, initial weights, etc) optimized via grid search. Training was stopped was when the network prediction accuracy reached 100% on unseen test data, after rounding the predictions to the nearest integer. The loss used to compute gradients for the optimizer was not rounded. In the results below, we deliberately use very large networks (12 layers with 100 neurons per layer) in order to ensure that the network has the capacity to represent the CA ruleset in as shallow or deep a manner as it finds—and we expect and observe that many fewer neurons per layer are used than are available. Consistent with prior reports that large networks approach a "mean field" limit [21–23], we find that training is highly repeatable for such large networks, even when different training data is used, different CA rules are learned, or the hyperparameters are altered slightly from their optimal values (although this extends the duration of training). We also find that doubling the depth and width of our networks does not qualitatively affect our results, consistent with a large-network limit. Additionally, we trained alternative networks using a different optimizer (vanilla stochastic gradient descent) and loss function (cross-entropy loss), and found nearly identical internal structure in the trained networks (as discussed below); however, the form of the loss curves during training was more concave for such networks. See the supplementary material for further details of networks and training.

Figure 2A shows the results of training a single network on the Game of Life, and then applying the trained network to the "glider," a known soliton-like solution to the Game. During the early stages of the training, the activations appear random and intermittent. As training proceeds, the network adjusts to the scale of output values generated by the input data, and then begins to learn clusters of related rules—leading to tightening of the output image and trimming of spurious activation patterns.

We consider the relevance of these observations to arbitrary binary cellular automata. Intuition would suggest that certain sets of CA rules are intrinsically easier to learn regardless of M and D; for example, a null CA that sends every input to zero in a single timestep requires a trivial network structure, while the Game of Life should require a structure like Figure 1 that can identify each possible neighborhood count. We thus repeat the training data generation and CA network training process described above, except this time we sample CA at random from the  $2^{2^9} \approx 10^{154}$  possible rulesets for binary CA. The complexity of the dynamics produced by a given rule are generally difficult to ascertain a priori, and typical efforts to systematically investigate the full CA rule space have focused on comparative simulations of different rules [16, 17]. For example, the Game of Life is a member of a unique set of "Class IV" CA capable of both chaotic and regular dynamics depending on their initial state; membership in this class has been hypothesized to be a prerequisite to supporting computational universality [15, 16]. General prediction of dynamical class is an ongoing question in the CA literature [19], however, there is known, approximate relationship between the complexity of simulated dynamics, and the relative fraction  $\lambda$  of transitions to zero and one among the full set of 512 possible input cases:  $\lambda = 0$  and  $\lambda = 1$  correspond to null CA, whereas  $\lambda = 0.5$  corresponds to CA that sends equal numbers of input cases to 0 and 1 [17]. This captures the general intuition that CA typically display richer dynamics when they have a broader range of output symbols [18]. Here, instead of using  $\lambda$  directly, we parametrize the space of CA equivalently using the effective "rule entropy,"  $\mathcal{H}_{ca}$ . We define  $\mathcal{H}_{ca}$  by starting from a maximum-entropy image with a uniform distribution of input symbols  $(p_{\sigma} \approx 1/M^D)$  for all  $\sigma$ ), to which we then apply the CA rule once and then record the new distribution of input cases,  $p'_{\sigma}$ . The residual Shannon entropy  $\mathcal{H}_{ca} \equiv -\sum_{\sigma} p'_{\sigma} \log_2 p'_{\sigma}$  provides a measure of the degree to which the CA rules compress the space of available states.  $\mathcal{H}_{ca}(\lambda)$  monotonically increases from  $\mathcal{H}_{ca}(0) = 0$ until it reaches a global maximum at  $\mathcal{H}_{ca}(1/2) = 9$ , after which it symmetrically decreases back to  $\mathcal{H}_{ca}(1) = 0$ .

Figure 2B shows the result of training 2560 randomly-sampled CA with different values of  $\mathcal{H}_{ca}$ . Ensembles of 512 related cellular automata were generated by randomly selecting single symbols in the input space to transition to 1 (starting with the null case  $\sigma \to 0$  for all  $\sigma$ ), one at a time, until reaching the case  $\sigma \to 1$  for all  $\sigma$ . This "table walk" sampling approach [17] was then replicated 5 times for different starting conditions.

We observe that the initial 10 - 100 training epochs are universal across  $\mathcal{H}_{ca}$ . Detailed analysis of the activation patterns across the network (Supplementary material) suggests that this transient corresponds to initialization, wherein the network learns the scale and bounds of the input data. During the next stage of training, the network begins to learn specific rules: the number of neurons activated in each layer begins to decrease, as the network becomes more selective regarding which inputs provoke non-zero network outputs (see supplementary material). Because  $\mathcal{H}_{ca}$  determines the sparsity of the rule table—and thus the degree to which the rules may be compressed— $\mathcal{H}_{ca}$  strongly affects the dynamics of this phase of training, with simpler CA learning faster and shallower representations of the rule table an, resulting in smaller final loss values (Figure 2B, inset). This behavior confirms general intuition that more complicated CA rules require more precise representations, making them harder to learn.

A key feature of using large networks to fit simple functions like CA is strong repeatability of training across different initializations and CA rulesets. Training with larger networks, or even with a different optimizer, loss function, and hyperparameters, creates nearly identical results. Such is not the case for "narrow" networks with fewer neurons per layer, for which training proceeds as a series of plateaus in the loss punctuated by large drops when the stochastic optimizer happens upon new rules. In this limit, randomly-chosen CA rulesets will not consistently result in training successfully finding all correct rules and terminating. Moreover, small networks that do terminate do not display apparent patterns when their internal structure is analyzed using the approaches described below—consistent with a random search. Similar loss dynamics have previously been observed when CA are learned using genetic algorithms, in which the loss function remains mostly flat, punctuated by occasional leaps when a mutant encounters a new rule [19]. For gradient-based training, similar kinetic trapping occurs in the vicinity of shallow minima or saddle points [27, 28], but these effects are reduced in larger networks such as those used here.

That training thousands of arbitrary CA yields extremely similar training dynamics suggests that deep networks trained using gradient optimizers learn a universal approach to approximating simple functions like CA. This motivates us to next investigate how exactly the trained networks represent the underlying CA rule table—do the networks simply match entire input patterns, or do they learn consolidated features such as

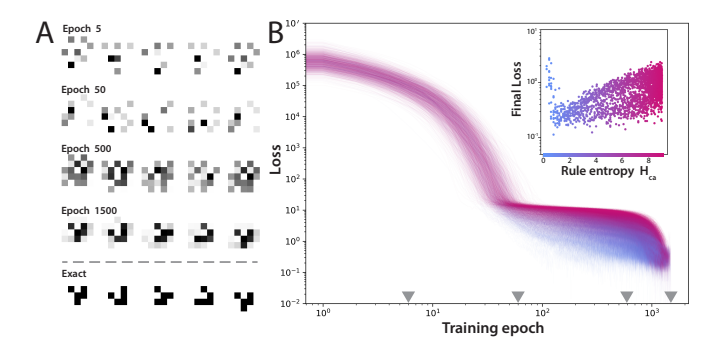


Figure 2. Training 2560 convolutional neural networks on random cellular automata. (A) Networks trained on the Game of Life for different durations, and then applied to images of each stage of the "glider" solution. (B) The loss versus time during training, colored by the rule entropy  $\mathcal{H}_{ca}$ . Groups of 512 related cellular automata were generated by iteratively choosing random  $\sigma \to 0$  rules from the 512 possible input configurations, and setting those sites to  $\sigma \to 1$ . 5 replicates were performed. The entropy of the resulting rule table is characteristic of the CA, and it is indicated by  $\mathcal{H}_{ca} = 0$  (blue, minimum entropy CA) to  $\mathcal{H}_{ca} = 9$  (magenta, maximum entropy CA). (Inset) The final loss for each network at the end of training, shown as a function of  $\mathcal{H}_{ca}$ .

neighbor counts? Because the intrinsic entropy of the CA rule table affects training, we reason that the entropy of activated representations at each layer is a natural heuristic for analyzing the internal states of the network. We thus define a binary measure of activity for each neuron in a fully-trained network: when the network encounters a given input  $\sigma$ , any neurons that produce a non-zero output are marked as 1 (or 0 otherwise), resulting in a new set of binary strings  $a(\sigma)$  denoting the rounded activation pattern for each input  $\sigma$ . For example, in an mlpconv network with only 3 layers, and 3 neurons per layer, an example activation pattern for a specific input  $\sigma_1$  could be  $a(\sigma_1) = \{010, 000, 011\}$ , with commas demarcating layers. Our approach constitutes a simplified version of efforts to study deep neural networks by inspecting activation pattern "images" of neurons in downstream layers when specific input images are fed into the network [22, 29–31]. However, for our system binary strings (thresholded activation patterns) are sufficient to characterize the trained networks, due to the finite space of input-output pairs for binary CA, and the large size of our networks; in our investigations, no cases were found in which two different inputs  $(\sigma, \sigma')$  produced different unrounded activation patterns, but identical patterns after binarization  $(a(\sigma), a(\sigma'))$ .

Given the ensemble of input symbols  $\sigma \in \{0, 1\}^D$ , and a network consisting of L layers each containing N neurons, we can define separate symbol spaces representing activations of the entire network  $a_T(\sigma) \in \{0, 1\}^{LN}$ ; each individual layer,  $a_{L,i}(\sigma) \in \{0, 1\}^N$ ,  $i \in [0, L]$ ; and each individual neuron  $a_{N,ij}(\sigma) \in \{0, 1\}$ ,  $i \in [0, L]$ ,  $j \in [0, N]$ . Averaging over test data consisting of an equiprobable ensemble of all  $M^D$  unique input cases  $\sigma$ , we can then

calculate the probability  $p_{\alpha,k}$  for observing a given unique symbol  $a_k$  at a level  $\alpha \in \{T, L, N\}$  in the network. We quantify the uniformity of each activation symbol distribution p using the entropy  $\mathcal{H}_{\alpha} = -\sum_{k} p_{\alpha,k} \log_2 p_{\alpha,k}$ , which satisfies  $\mathcal{H}_{\alpha} \leq \dim(\alpha)$ . We condense notation and refer to the activation entropies  $\mathcal{H}_T$ ,  $\mathcal{H}_{L,i}$ ,  $\mathcal{H}_{N,ij}$  as the total entropy, the entropy of  $i^{th}$  layer, and the entropy of the  $j^{th}$  neuron in the  $i^{th}$  layer. We note that, in addition to readily quantifying the number of unique activation patterns and their uniformity across input cases, the Shannon entropy naturally discounts zero-entropy "dead neurons," a common artifact of training high-dimensional ReLU networks [26].

We expect and observe that  $\langle \mathcal{H}_{N,ij} \rangle_{ij} < \langle \mathcal{H}_{L,i} \rangle_i \leq \mathcal{H}_T$ . Unsurprisingly, the maximum entropy of a single neuron is  $\log_2 2 = 1$ , and all multi-neuron layers generate more than two patterns across the test data. We also observe that  $\mathcal{H}_T \approx 9$  for all networks trained, suggesting that the overall firing patterns in the network differed for every unique input case—even for trivial rules like  $\lambda = 0$ where a network with all zero weights and biases would both correctly represent the rule table, and have identical firing patterns for all inputs ( $\mathcal{H}_T = 0$ ). This effect directly arises from training using gradient-based methods, for which at least some early layers in the network produce unique activation patterns for each  $\sigma$  that are never condensed during later training stages. Accordingly, regularization using a total weight cost or dropout both reduce  $\mathcal{H}_T$ .

Comparing  $\mathcal{H}_{L,i}$  across models and layers demonstrates that early layers in the network tend to generate a broad set of activation patterns that closely follow the uniform input symbol distribution (Figure 3A). These early layers in the network thus remain saturated at  $\mathcal{H}_{L,i} = \mathcal{H}_T \approx 9$ ; however in deeper layers progressively lower entropies are observed, consistent with fewer unique activation patterns (and a less uniform distribution across these strings) appearing in later layers. These trends depend strongly on the CA rules (coloration). In the figure, dashed lines allow comparison of  $\mathcal{H}_{L,i}$  to theoretical predictions for the layerwise entropy for the different types of ways that a CNN can represent the CA. The uppermost dashed curve corresponds to a network that generates a maximum entropy set of 512 equiprobable activation patterns in each layer. This case corresponds to a "shallow" network that matches each input case to a unique template at each layer. Lower dashed curves correspond to predictions for networks that implement the CA as layerwise search, in which  $\sigma$  that map to the same output m are mapped to the same activation pattern at some point before the final layer. This corresponds to a progressive decrease in the number of unique activation patterns in each layer. The two dashed curves shown correspond to theoretical networks that eliminate 45% and 50% of unique activation patterns at each layer.

We find that higher entropy rules  $\mathcal{H}_{ca}$  (red points) tend to produce shallower networks due to the rule table being less intrinsically compressible; whereas simpler

CA (blue points) produce networks with more tree-like structure. This relationship has high variance in early layers, making it difficult to visually discern in the panel save for the last layer. However, explicit calculation of the Pearson correlation  $r(\mathcal{H}_{ca}, \mathcal{H}_{L,i})$  confirms its presence across all layers of the network, and that it becomes more prominent in deeper layers (Figure 3A, inset). This trend is a consequence of training the network using backpropagation-based techniques, in which loss gradients computed at the final,  $L^{th}$  hidden layer are used to update the weights in the previous  $(L-1)^{th}$  layer, which are then used to update the  $(L-2)^{th}$  layer, and so forth [32]. During training, the entropy of the final layer increases continuously until it reaches a plateau determined by the network size and by  $\mathcal{H}_{ca}$ . The penultimate layer then increases in entropy until reaching a plateau, and so forth until  $\mathcal{H}_T = 9$  across all  $\sigma$ —at which point training stops because the test error will reach zero (training dynamics are further analyzed in the Supplementary Material).

The role of  $\mathcal{H}_{ca}$  on internal representation distributions  $p_L$  can be further analyzed using Zipf plots of activation pattern  $a_k$  frequency versus rank (Supplementary Material): the resulting plots show that the distribution of activation symbols is initially uniform (because the training data has a uniform distribution of  $\sigma$ ), but the distribution becomes progressively narrower and more peaked in later layers. This process occurs more sharply for networks trained on CA with larger  $\mathcal{H}_{ca}$ .

We next consider how our observed layer activation patterns result from the entropy of the individual neurons  $\mathcal{H}_{N,ij}$  that comprise them; we suspect there is a relation because the individual firing entropies determine the "effective" number of neurons in a layer,  $N_{\text{eff}} = 2^{\sum_{j} \mathcal{H}_{N,ij}}$ . Across all layers, we observe a linear relationship between  $\mathcal{H}_{N,ij}$  and  $\mathcal{H}_{L,i}$  that saturates when  $\mathcal{H}_{L,i} \approx \mathcal{H}_T$  (Figure 3B). The lower- $\mathcal{H}_{ca}$  CA lie within the linear portion of this plot, suggesting that variation in activation patterns in this regime results from layers recruiting varying numbers of neurons. Conversely, higher-entropy CA localize in a saturated region where each layer encodes a unique activation pattern for each unique input state, leading to no dependence on the total effective number of neurons. This plot explains our earlier observation that the dynamics of training do not depend on the exact network shape as long as the network has sufficiently many neurons: for low  $\mathcal{H}_{ca}$ , layers never saturate, and are free to recruit more neurons until they are able to pattern-match every unique input (at intermediate and large  $\mathcal{H}_{ca}$ ). A CA with more possible input states (larger M or D) would thus require more neurons per layer to enter this large-network limit.

We also consider the degree to which the decrease  $\mathcal{H}_{L,i}$  vs. i arises from deeper layers becoming "specialized" to specific input features, a common observation for deep neural networks [12, 30, 32]. We quantify the layer specialization using the total correlation, a measure of the mutual information between the acti-

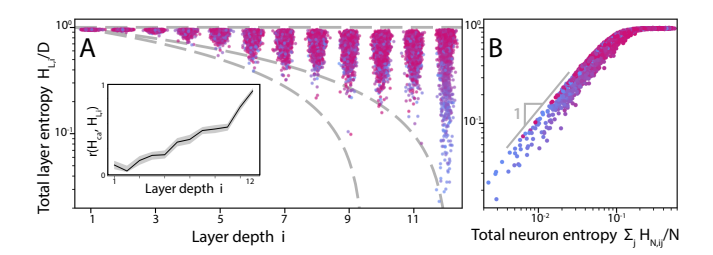


Figure 3. Internal representations of cellular automata by trained networks. (A) The individual layerwise entropy  $(\mathcal{H}_{L,i}/D)$  for the 2560 networks shown in the previous figure. Noise has been added to the horizontal coordinates (layer index) to facilitate visualization. As in previous figures, coloration corresponds to the entropy  $\mathcal{H}_{ca}$  of the underlying CA. Dashed lines correspond to expected trends for theoretical networks that eliminates 0% of cases in each layer (i.e., a pattern-matching implementation), 45% of cases, and 50%(top to bottom) (Inset) The Pearson correlation coefficient rbetween the rule entropy  $\mathcal{H}_{ca}$  and layer entropy  $\mathcal{H}_{L,i}$ . Error range corresponds to bootstrapped 25% -75% quantiles. (B) The normalized layerwise entropy  $(\mathcal{H}_{L,i}/D)$  versus the normalized total layerwise neuron entropy  $(\mathcal{H}_{N,ij}/N)$ , with the linear scaling annotated.

vation patterns of a layer, and the neurons within that layer:  $\mathcal{I}_i = \sum_j \mathcal{H}_{N,ij} - \mathcal{H}_{L,i}$ . This quantity is minimized  $(\mathcal{I}_i = 0)$  when the single neuron activations within a layer are independent of one another; conversely, at the maximum value individual neurons only activate jointly in the context of forming a specific layer activation pattern. Plots of  $\mathcal{I}_i$  vs. i (Supplementary material) reveal that during early stages of training, individual neurons tend to fire independently, consistent with multi-neuron features being unique to each input case. In these early layers,  $\mathcal{I}_i$  is large because the number of possible activation patterns in a single layer of the large network  $(2^{100})$ is much larger than the number of input cases  $(2^9)$ . In later layers, however, the correlation begins to decrease, consistent with individual neurons being activated in the context of multiple input cases—indicating that these neurons are associated with features found in multiple input cases, like the states of specific neighbors. Calculation of  $r(\mathcal{I}_i, \mathcal{H}_{ca})$  confirms that this effect varies with

We have shown an analogy between convolutional neural networks and cellular automata, and demonstrated a type of network capable of learning arbitrary binary CA using standard techniques. Our approach uses a simple architecture that applies repeated  $1 \times 1$  convolutions to perform local operations, and which predicts output states using a mixture of shallow pattern-matching and deep layer-wise tree searching. After training an ensemble of networks on a variety of CA, we find that our networks structurally encode generic dynamical features of CA, such as the relative entropy of the rule table. Further work is necessary to determine whether neural networks can more broadly inform efforts to understand the dynamical space of CA, including fundamental efforts to

relate a CA's a priori rules to the its apparent dynamical complexity during simulation [16, 18, 20]—for example, do Class IV and other complex CA impose unique structures upon fitted neural networks, or can neural networks predict their computational complexity given a rule table? These problems and more general studies of dynamical systems will require more sophisticated approaches, such as unsupervised training and generative architectures (such as restricted Boltzmann machines). More

broadly, we note that studying the bounded space of CA has motivated our development of general entropy-based approaches to probing trained neural networks. In future work we hope to relate our observations to more general patterns observed in studies of deep networks, such as the information bottleneck [33]. Such results may inform analysis of open-ended dynamical prediction tasks, such as video prediction, by showing a simple manner in which process complexity manifests as structural motifs.

- [1] L. Zdeborová, Nature Physics **13**, 420 (2017).
- [2] J. Pathak, B. Hunt, M. Girvan, Z. Lu, and E. Ott, Physical review letters 120, 024102 (2018).
- [3] J. Carrasquilla and R. G. Melko, Nature Physics 13, 431 (2017).
- [4] E. P. Van Nieuwenburg, Y.-H. Liu, and S. D. Huber, Nature Physics 13, 435 (2017).
- [5] G. Torlai, G. Mazzola, J. Carrasquilla, M. Troyer, R. Melko, and G. Carleo, Nature Physics 14, 447 (2018).
- [6] H. Jaeger and H. Haas, science 304, 78 (2004).
- [7] Y. Bar-Sinai, S. Hoyer, J. Hickey, and M. P. Brenner, arXiv preprint arXiv:1808.04930 (2018).
- [8] J. N. Kutz, Journal of Fluid Mechanics 814, 1 (2017).
- [9] G. Carleo and M. Troyer, Science **355**, 602 (2017).
- [10] G. Torlai and R. G. Melko, Physical Review B 94, 165134 (2016).
- [11] P. Zhang, H. Shen, and H. Zhai, Physical review letters 120, 066401 (2018).
- [12] Y. LeCun, Y. Bengio, and G. Hinton, nature **521**, 436 (2015).
- [13] A. Van Den Oord, S. Dieleman, H. Zen, K. Simonyan, O. Vinyals, A. Graves, N. Kalchbrenner, A. W. Senior, and K. Kavukcuoglu, in SSW (2016) p. 125.
- [14] M. Mathieu, C. Couprie, and Y. LeCun, arXiv preprint arXiv:1511.05440 (2015).
- [15] A. Adamatzky, Game of life cellular automata, Vol. 1 (Springer, 2010).
- [16] S. Wolfram, Reviews of modern physics 55, 601 (1983).
- [17] C. G. Langton, Physica D: Nonlinear Phenomena **42**, 12 (1990).
- [18] D. P. Feldman, C. S. McTague, and J. P. Crutchfield, Chaos: An Interdisciplinary Journal of Nonlinear Science 18, 043106 (2008).
- [19] M. Mitchell, J. P. Crutchfield, R. Das, et al., in Proceedings of the First International Conference on Evolutionary Computation and Its Applications (EvCA?96), Vol. 8 (Moscow, 1996).

- [20] M. Mitchell and P. T. Hraber, Complex Systems 7, 89 (1993).
- [21] R. M. Neal, Bayesian learning for neural networks, Vol. 118 (Springer Science & Business Media, 2012).
- [22] M. Chen, J. Pennington, and S. S. Schoenholz, arXiv preprint arXiv:1806.05394 (2018).
- [23] H. Sompolinsky, A. Crisanti, and H.-J. Sommers, Physical review letters 61, 259 (1988).
- [24] C. Szegedy, W. Liu, Y. Jia, P. Sermanet, S. Reed, D. Anguelov, D. Erhan, V. Vanhoucke, and A. Rabinovich, in *Proceedings of the IEEE conference on com*puter vision and pattern recognition (2015) pp. 1–9.
- [25] M. Lin, Q. Chen, and S. Yan, arXiv preprint arXiv:1312.4400 (2013).
- [26] V. Nair and G. E. Hinton, in Proceedings of the 27th international conference on machine learning (ICML-10) (2010) pp. 807–814.
- [27] D. Saad and S. A. Solla, Physical Review E 52, 4225 (1995).
- [28] Y. N. Dauphin, R. Pascanu, C. Gulcehre, K. Cho, S. Ganguli, and Y. Bengio, in *Advances in neural information processing systems* (2014) pp. 2933–2941.
- [29] S. S. Schoenholz, J. Gilmer, S. Ganguli, and J. Sohl-Dickstein, in *International Conference on Machine Learning* (2017).
- [30] D. Erhan, Y. Bengio, A. Courville, and P. Vincent, University of Montreal **1341**, 1 (2009).
- [31] B. Poole, S. Lahiri, M. Raghu, J. Sohl-Dickstein, and S. Ganguli, in Advances in neural information processing systems (2016) pp. 3360–3368.
- [32] S. Arora, A. Bhaskara, R. Ge, and T. Ma, in *International Conference on Machine Learning* (2014) pp. 584–592.
- [33] R. Shwartz-Ziv and N. Tishby, arXiv preprint arXiv:1703.00810 (2017).